Document downloaded from:

http://hdl.handle.net/10251/107385

This paper must be cited as:

Verdia-Baguena, C.; Gómez Lozano, V.; Cervera, J.; Ramirez Hoyos, P.; Mafe, S. (2017). Energy transduction and signal averaging of fluctuating electric fields by a single protein ion channel. Physical Chemistry Chemical Physics. 19(1):292-296. doi:10.1039/c6cp06035h

The final publication is available at

https://doi.org/10.1039/c6cp06035h

Copyright The Royal Society of Chemistry

Additional Information

Please do not adjust margins

Journal Name

ARTICLE

Energy transduction and signal averaging of fluctuating electric fields by a single protein ion channel

Received 00th January 20xx,
Accepted 00th January 20xx

DOI: 10.1039/x0xx00000x

www.rsc.org/

C. Verdia-Baguena,[a] V. Gomez,[b] J. Cervera,[c] P. Ramirez[b]* and S. Mafe[c]

We demonstrate the electrical rectification and signal averaging of fluctuating signals using a biological nanostructure in aqueous solution: a single protein ion channel inserted in the lipid bilayer characteristic of cell membranes. The conversion of oscillating, zero time-average potentials into directional currents permits to charge a load capacitor to significant steady-state voltages within a few minutes in the case of the *Outer membrane porin F* (OmpF) protein, a bacterial channel of *Escherichia coli*. The experiments and simulations show signal averaging effects at a more fundamental level than the traditional cell and tissue scales which are characterized by ensembles of many ion channels operating simultaneously. The results suggest also signal transduction schemes with bio-electronic interfaces and ionic circuits where soft matter nanodiodes can be coupled to conventional electronic elements.

1. Introduction

Directional fluxes of energy and information occur in the highly fluctuating environment characteristic of biological nanostructures. This is the case of the ion channels in cell membranes, the protein aqueous pores which allow the transmission and processing of noisy electrical signals.[1] The coexistence of net currents and noise is also significant for developing applications at the nanoscale where fluctuations are usually regarded as a nuisance, not as an opportunity. While the correlation between fluctuations and the state of a system cannot give net currents from equilibrium random fluctuations, this is not the case of non-equilibrium external fluctuations which are uncorrelated to the system state.[2]

It is of wide interest to demonstrate experimental methods allowing the conversion of randomly fluctuating external signals into directional average responses using nanostructures. Previous studies by Siwy[3] and us[2] have considered the conversion of zero time-average electrical signals into net currents using artificial nanopores. With respect to our previous work,[2] the following significant differences should be emphasized: i) we study here a biological nanoscale system: the Outer membrane porin F (OmpF) protein, a bacterial ion channel of Escherichia coli, instead of an artificial polymeric conical nanopore; ii) the single protein is inserted in the lipid bilayer characteristic of cell membranes[1,4] and we use different experimental techniques and equipment because ion channel net currents (pA) are much lower than nanopore currents (nA); iii) the dimensions of the OmpF protein are of the order of a few nm in radii and length while those of the synthetic conical nanopores used in previous experiments are of the order of ten nm (pore tip), hundreds of nm (pore base) and ten μm (length); iv) we demonstrate that ion channels can be coupled efficiently with conventional circuit elements, yielding bio-electronic schemes that work in a reproducible and predictable way, which could be exploited in the design of signal averaging and energy transduction schemes using nanopore-based ionic circuits;[5-13] v) the synthetic nanopores used in our previous experiments[2] operate in the range of 1 – 3 V, while the OmpF protein used here show similar current rectifications in the range of 100 – 150 mV, thus decreasing the noise voltages needed to charge the capacitor in one order of magnitude; and, finally, vi) we show that low frequency zero time-average electromagnetic fields could produce noticeable accumulative effects in single ion channels.

Note also that single protein experiments could permit to quantify the signal averaging of fluctuating fields at a more fundamental level than the traditional cell and tissue scales,[14] which involve ensembles of many ion channels operating simultaneously. Ion channel selectivity and electric field-sensing are crucial to bioelectrical activity.[15,16] Oscillating electrical signals are also observed along the cell cycle[17] and in intercellular communication.[18-20] The bioelectrical characteristics of commercially available protein ion channels and toxin pore-formers can be used in bio-electronic interfaces and ionic nanodevices;[4-7,17] in particular, asymmetric channels allow different electrical rectification phenomena.[4,21-23]

[a] Dept. de Física, Universitat Jaume I de Castelló, E-12080 Castelló, Spain
[b] Departament de Física Aplicada, Universitat Politècnica de València, E-46022 València, Spain. E-mail: patraho@fis.upv.es
[c] Dept. de Física de la Tierra i Termodinàmica, Universitat de València, E-46100 Burjassot, Spain

Please do not adjust margins

Please do not adjust margins

2. Experimental methods

2.1 Materials

The single OmpF porin reconstituted on a planar diphytanoylphosphatidylcholine (DPhPC) lipid bilayer (Avanti Polar Lipids, Alabaster, AL) separates two 0.1 M KCl aqueous solutions. The reconstitution procedure can be found elsewhere.[22] When $pH_L = 3$ and $pH_R = 12$, where L denotes the side of protein addition, the protein channel acts as a biological nanofluidic diode because of the positive (basic) residues on the left side and the negative (acidic) residues on the right side.[4] The resulting fixed charge asymmetry along the protein channel leads to the observed rectifying characteristics in the current (I) – voltage (V) curve. The symmetrical case $pH_L = pH_R = 6$ gives a quasi-ohmic behavior.

2.2 Electrical measurements

The case $V > 0$ corresponds to the electric potential being higher at the L side than at the R side of the membrane cell. The current $I > 0$ corresponds to an electric flow from the L solution to the R solution. Voltage and current are measured with an Axopatch 200B amplifier (Molecular Devices, Sunnyvale, CA). Ag|AgCl electrodes are used in the L and R solutions to externally apply the fluctuating potentials. A WW5062 Tabor Electronics wave generator was used to introduce the random noise signals (25 MHz bandwith). The voltage across the load capacitor is measured with an electrometer (Keithley 6514, input impedance > 200 TΩ, sampling frequency 50 kHz). The electrochemical cell with the lipid bilayer is confined within a double layer magnetic shield (Amuneal Manufacturing, Philadelphia, PA) to avoid external perturbations. The system formed by the single channel inserted in the lipid bilayer has an effective capacitance of the order of 100 pF. Occasionally, two channels instead of one can be inserted in the lipid bilayer, which can be readily detected by the anomalies observed in the time traces for $V_C(t)$ during the charging process. In this case, the capacitor charging is still possible but the time constants obtained are not characteristic of the single protein case we wish to study here.

Results and discussion

Fig. 1a schematically shows the single ion channel protein reconstituted on a planar lipid bilayer which separates two aqueous KCl solutions of concentrations $c_L = c_R = 0.1$ M. The electrical charge of the basic and acidic protein residues distributed along the channel axis depends on their ionization state. The preference of the channel for cations or anions (ionic selectivity) is dictated by the solution pH:[21,22] the positively charged channel is selective to anions at low pH whereas the negatively charged channel is selective to cations at high pH. Not only the ion selectivity but also the I–V curves in Fig. 1b are dictated by the pH values in the external solutions.[4] The asymmetric configuration case ($pH_L \neq pH_R$) gives nonlinear I–V curves (rectifying behaviour, with a high conducting regime for $V > 0$ and a low conducting regime for $V < 0$) while the symmetrical case ($pH_L = pH_R$) gives quasi-linear I–V curves (Figs. 1c and 1d). In the asymmetric case, the Nernst voltage offset is negligible because of the relatively high concentration of KCl (0.1 M) compared with the water ions concentration.[1]

The channel ionic current is dictated by the potassium and chloride ions in the pore aqueous solution because these ions have concentrations much higher than those of hydrogen and hydroxyl ions under the conditions in Figs. 1a and 1c. The water ions allow the biological nanostructure to show a bipolar distribution of fixed charges (Fig. 1a) but do not add a significant contribution to the total current.[4,22] The asymmetric charge distribution along the protein pore in Fig. 1a gives the rectification characteristics of the nanofluidic diode in Fig. 1b. The rectification ratio, defined as the ratio of the high conducting regime to the low conducting regime currents and measured at the same absolute value of the voltage, describes the performance of the diode as a rectifier. In the case of the asymmetric configuration of Fig. 1b, the rectification ratio is about 7 at 150 mV. In the synthetic nanopores used in previous experiments,[2] applied voltages in the range 1 – 3 V were needed to obtain similar rectification ratios.

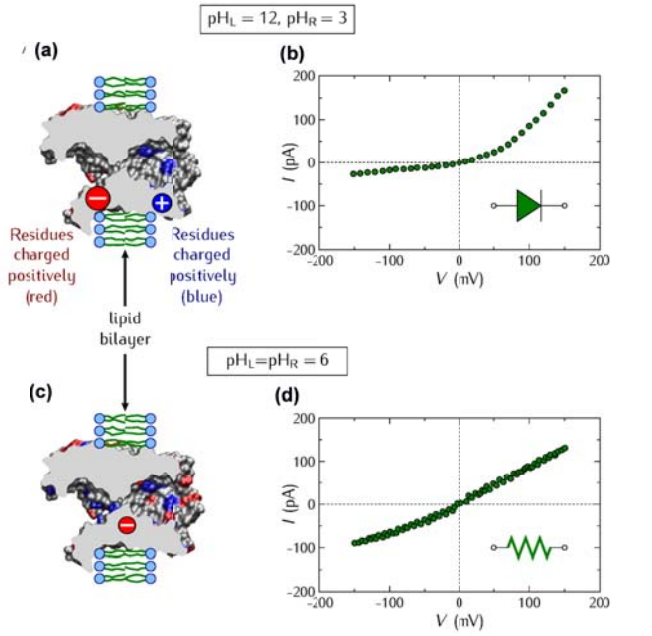

Fig. 1 (a) The porin reconstituted on a planar lipid bilayer separates two aqueous KCl solutions of concentrations $c_L = c_R = 0.1$ M, with $pH_L = 12$ and $pH_R = 3$. The positively charged basic residues (in blue) and negatively charged acidic residues (in red) are highlighted in the resulting bipolar nanostructure. (b) The electrical rectification in the steady-state I–V curve results from the asymmetric fixed charge distribution along the protein axis produced by the different pH conditions in the external solutions. (c) and (d) The control experiment showing decreased electrical rectification for the symmetric case $pH_L = 6 = pH_R$.

Fig. 2 (top) shows the experimental set-up for the charging process. The electrochemical cell that contains the planar lipid bilayer and the load capacitor of capacitance C connected in series to the protein channel are electromagnetically shielded from external noises. Fig. 2 (left) shows the randomly fluctuating electric potential $V_{in}(t)$ of zero time-average (white

This journal is © The Royal Society of Chemistry 20xx

Please do not adjust margins

Please do not adjust margins

noise) applied externally. The oscillating input signal is characterized by the voltage amplitude V_0 and the pulse 0.01 s. The pore rectification shown in Fig. 1b gives the output electric current $I_{out}(t)$ in Fig. 2 (bottom). The instantaneous current $I_{out}(t)$ shows no time delay with respect to $V_{in}(t)$ because the input potential period is much longer than the typical relaxation time of the system[4,23] (note the small volume available for ionic conduction within the protein pore of Fig. 1a).

A capacitor voltage $V_C(t)$ is set up in Fig. 2 (right) due to the non-zero average current obtained with the oscillating signal in Fig. 2 (left). Because this voltage drives a reverse current which opposes to the charging process, the total current decreases to zero when the capacitor approaches the final voltage $V_C(\infty)$ for large times $t \to \infty$.

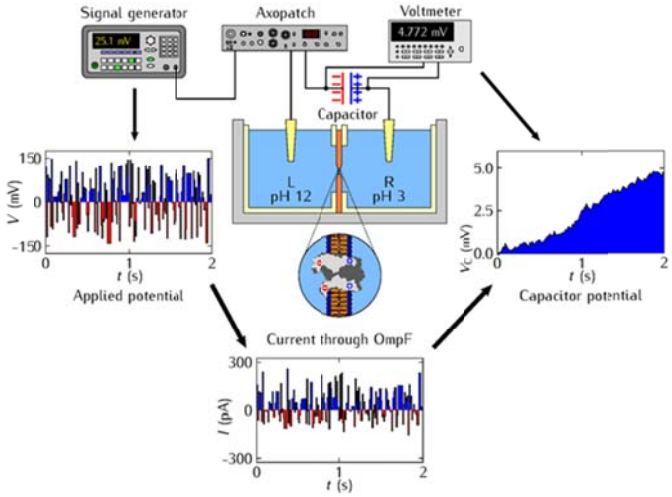

Fig. 2 Scheme of the charging experiment (top): a load capacitor of capacitance C connected in series to the single protein inserted in the lipid bilayer is charged because of the ion channel electrical rectification. The fluctuating electric potential $V_{in}(t)$ of zero time-average (left) is externally applied with a signal generator acting as a voltage source. The resulting output current $I_{out}(t)$ through the ion channel (bottom) has a non-zero average value. This signal averaging effect results in the net current that gives the instantaneous capacitor voltage potential difference $V_C(t)$ (right).

Fig. 3a shows the typical time traces measured for the capacitor voltage V_C(t) during the charging process for a capacitance C = 100 nF. The curves are parametric in the amplitude V_0 of the input fluctuating potential. For potential amplitudes in the range of 50–150 mV, the single protein rectification of an external oscillating signal gives significant steady-state capacitor voltages within a few minutes.

Fig. 3b shows the discharging process obtained for the amplitude V_0 = 150 mV in Fig. 3a when the external potential is switched off. Fig. 1a suggests a pore resistance of the order of 1 GΩ. For a load capacitance C = 100 nF, the characteristic time of the electrical circuit should then be of the order of 10^9 Ω×10^{-7} F = 100 s, which is in agreement with the results of Figs. 3a and 3b. Note that the rectification in Fig. 1b can lead to different single channel resistances for the charging and discharging processes.

To check further that the capacitor charging process is due to the single protein rectification, Fig. 3c considers a broad range of capacitances, C = 1–100 nF. As expected the charging time increases with the capacitance. However, high enough capacitance values are required to characterize accurately the capacitor voltage, as shown in Fig. 3c. Indeed, a balance should be reached between the charging time and the capacitor voltage determination. Remarkably, significant accumulative effects resulting in a high value of V_C can be obtained within a few seconds for the low capacitance case.

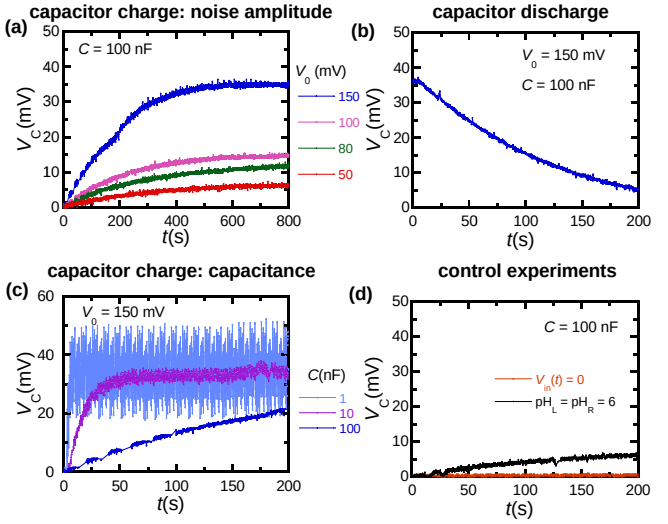

Fig. 3 (a) Time traces for the capacitor voltage $V_C(t)$ during the charging process with a capacitance C = 100 nF in Fig. 2. The curves are parametric in the amplitude V_0 of the fluctuating potential. (b) The discharging process for $V_C(t)$ in the case V_0 = 150 mV in Fig. 3a. (c) Time traces for $V_C(t)$ during the charging process parametric in the capacitances C = 100 nF, 10 nF and 1 nF. (d) The control experiments correspond to the absence of external signals ($V_{in}(t)$ = 0) and to the symmetric pH case in Fig. 1d for V_0 = 100 mV.

Fig. 3d shows two control experiments corresponding to the absence of externally applied signal ($V_{in}(t)$ = 0) and to the symmetric pH case of Fig. 1d. The bottom curve in Fig. 3d shows that the capacitor voltage is close to 1 mV in absence of external oscillating signals, which is a value significantly lower than most of the observed potentials in Fig. 3a. This result demonstrates that the charging process results from the rectification of the external fluctuating signal by the single protein channel and is not influenced by other noise sources due to the electrical equipment. The top curve in Fig. 3d emphasizes the importance of the rectification shown in Figs. 1b and 1d: when the protein exhibits quasi-ohmic behavior, the charging process is noticeably reduced. As to the charging process efficiency, it can be estimated from the energy ratio[2]

$$e \equiv \frac{1}{2} C V_C(\infty)^2 / \int_0^T I_{out}(t) V_{in}(t) dt \qquad (1)$$

The experimental results of Fig. 3a suggest an effective time $T = 3\tau_{ch}$ for the maximum capacitor voltage, where τ_{ch} is the

Please do not adjust margins

Please do not adjust margins

characteristic charging time. From the recorded experimental data, the above energy ratio is of the order of 1%.

By assuming that the channel is a potential dependent resistor connected in series with the capacitor, the charging process can be simulated. When the circuit is fed with an oscillating potential of amplitude V_0, the charging process is described by the equation

$$dV_C(t)/dt = I_{out}(t)/C \quad (2)$$

We fix a constant time step Δt for the potential $V_{in}(t)$ to take random values distributed between $-V_0$ and $+V_0$ and introduce the initial condition $V_C(t = 0) = 0$. The capacitor voltage is then updated as $V_C \rightarrow V_C + I(V)\Delta t/C$, where $I(V)$ is read from the measured I–V curve in Fig. 1b, to obtain the final maximum voltage $V_C(\infty)$. The discharging process can be simulated by introducing $V_{in}(t) = 0$ in the numerical algorithm. The theoretical simulations of Figs. 4a and 4b are parametric in the noise amplitude and capacitance. The model results can describe the observed behavior, giving further support to the experimental charging process.

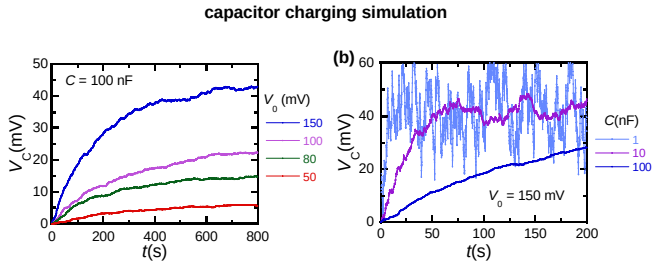

Fig. 4 (a) Time traces for the simulated capacitor voltage $V_C(t)$ during the charging process with C = 100 nF. The curves are parametric in the amplitude V_0 of the oscillating potential. (b) Simulated charging curves for the capacitances in Fig. 3c and V_0 = 150 mV.

Fig. 5a (experiment) and Fig. 5b (simulation) show the frequency response of the capacitor charging curve for the case of a sinusoidal input voltage. The capacitor voltage oscillates at low frequencies because of the increased coupling with the input signal compared with the high frequency case. The theoretical simulations can approximately describe the observed results.

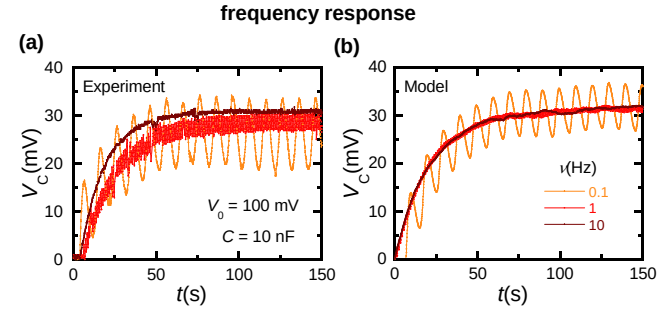

Fig. 5 (a) The experimental capacitor charging curves for sinusoidal input voltages of frequencies 0.1, 1, and 10 Hz with C = 10 nF and V_0 = 100 mV. (b) The simulation curves.

Taken together, Figs. 2-5 demonstrate that the electrical rectification provided by a single ion channel inserted in a lipid bilayer is able to convert zero time-average signals into directional currents which allow charging a conventional electronic element. These results must not be extrapolated to the single cell case because of the increased complexity involved in this change of scale and the multitude of ion channels present in the biological membrane.[1]

However, the present experimental approach should have wide interest: the protein ion channels constitute the building blocks of the cell membrane electrical network and are also involved in the design of ionic circuits for bio-electronic interfaces and nanofluidic sensors. While external amplitudes of tens of millivolts may be larger than those likely to arise from most environmental sources, they are typical of the electrical signals found in the cell cycle[16] and intercellular communication,[17] bio-nanoelectronic interfaces,[24] bioinspired sensing nanochannels,[5,6,25] and bio-electrochemical cells.[26] Note also that the artificial nanostructures should be effectively coupled to conventional electronic elements such as capacitors to achieve full functionality and short-time responses.

Conclusions

Oscillating fields and membrane potentials are of interest to biophysical processes based on protein ion channels.[16-18] A protein pore with an asymmetric charge distribution constitutes a soft matter nanostructure which can mimic the electrical characteristics of macroscopic solid-state diodes.[27] By rectifying randomly fluctuating signals of amplitudes in the range of tens of millivolts, this biological pore permits to charge a commercial capacitor to significant voltages within minutes. The protein channel is inserted in the lipid bilayer characteristic of cell membranes and operates in aqueous salt solutions.[1,17] The described experimental approach suggest new methods to quantify the signal averaging of low frequency oscillating signals at a more fundamental level than the traditional cell and tissue scales.[14]

There are different, commercially available ion channel and toxin pore-formers (e.g. gramicidin A and alpha-hemolysin). The results show an efficient coupling between these biological nanostructures and conventional capacitors. This coupling can be of interest for the design of signal averaging and energy transduction schemes using bio-electronic interfaces and nanopore-based ionic circuits where miniaturization leads to novel properties.[5-9] Also, the significant charging effects observed suggest that noisy zero-average signals could produce noticeable accumulative results in highly rectifying ion channels.

Acknowledgements

We acknowledge the support from the Ministry of Economic Affairs and Competitiveness and FEDER (project MAT2015-65011-P) and the Generalitat Valenciana (project Prometeo/GV/0069). We thank Profs. A. Alcaraz and V. M.

This journal is © The Royal Society of Chemistry 20xx

Please do not adjust margins

Please do not adjust margins

Aguilella for fruitful suggestions. This paper is devoted to the memory of Professor Kyösti Kontturi, Aalto University, Finland.

Notes and references

1 B. Hille, Ionic Channels of Excitable Membranes, Sinauer, Sunderland, 1992.
2 V. Gomez, P. Ramirez, J. Cervera, S. Nasir, M. Ali, W. Ensinger and S. Mafe, *Sci. Rep.*, 2015, **5**, 9501-9505.
3 Z. Siwy and A. Fulinski, *Phys. Rev. Lett.*, 2002, **89**, 198103.
4 M. Queralt-Martín, M. E. García-Giménez, V. M. Aguilella, P. Ramirez, S. Mafe and A. Alcaraz, *Appl. Phys. Lett.*, 2013, **103**, 043707.
5 K. Xiao, L. Wen and L. Jiang, *Small*, 2016, 3, 3339-3342.
6 Q. Liu, L. Wen, K. Xiao, H. Lu, Z. Zhang, G. Xie, X.-Y. Kong, Z. Bo and L. Jiang, *Adv. Mater.*, 2016, **28**, 3181-3186.
7 N. Misra, J. A. Martinez, S.-C. J. Huang, Y. Wang, P. Stroeve, C. P. Grigoropoulos and A. Noy, *Proc. Natl. Acad. Sci. U.S.A.*, 2009, **106**, 13780-13784.
8 P. Ramirez, M. Ali, W. Ensinger and S. Mafe, *Appl. Phys. Lett.*, 2012, **101**, 133108.
9 K. Tybrandt, R. Forchheimer and M. Berggren, *Nat. Commun.*, 2012, **3**, 871.
10 V. Gomez, J. Cervera, S. Nasir, M. Ali, W. Ensinger, S. Mafe and P. Ramirez, *Electrochem. Commun.*, 2016, **62**, 29-33.
11 W. Guo, L. Cao, J. Xia, F.-Q. Nie, W. Ma, J. Xue, Y. Song, D. Zhu, Y. Wang and L. Jiang, *Adv. Funct. Mater.*, 2010, **20**, 1339-1344.
12 J. Gao, W. Guo, D. Feng, H. Wang, D. Zhao and L. Jiang, *J. Am. Chem. Soc.*, 2014, **136**, 12265-12272.
13 W. Guo, Y. Tian and L. Jiang, *Acc. Chem. Res.*, 2013, **12**, 2834-2846.
14 M. Hronik-Tupaj and D. L. Kaplan, *Tissue Eng. B*, 2012, **18**, 167-180.
15 D. J. Blackiston, K. A. McLaughlin and M. Levin, *Cell Cycle*, 2009, **8**, 3527-3536.
16 M. Levin, *Bioessays*, 2012, **34**, 205-217.
17 F. Chang and N. Minc, *Annu. Rev. Cell Dev. Biol.*, 2014, **30**, 317-336.
18 J. Cervera, J. A. Manzanares and S. Mafe, *J. Phys. Chem. B*, 2015, **119**, 2968-2978.
19 B. T. Chernet and M. Levin, *J. Clin. Exp. Oncol.*, 2013, Supl 1, S1-002.
20 M. Levin, *Wiley Interdiscip. Rev. Syst. Biol. Med.*, 2013, **5**, 657-676.
21 A. Alcaraz, E. M. Nestorovich, M. Aguilella-Arzo, V. M. Aguilella and S. M. Bezrukov, *Biophys. J.*, 2004, **87**, 943-957.
22 Alcaraz, P. Ramírez, E. García-Giménez, M. L. López, A. Andrio and V. M. Aguilella, *J. Phys. Chem. B*, 2006, **110**, 21205-21209.
23 Verdiá-Báguena, M. Queralt-Martín, V. M. Aguilella and A. Alcaraz, *J. Phys.Chem. C*, 2012, **116**, 6537-6542.
24 A. Noy, *Adv. Mater.*, 2011, **23**, 807-820.
25 M. Ali, S. Nasir, P. Ramirez, J. Cervera, S. Mafe and W. Ensinger, *J. Phys. Chem. C*, 2013, **117**, 18234-18242.
26 O. Yehezkeli, R. Tel-Vered, J. Wasserman, A. Trifonov, D. Michaeli, R. Nechushtai and I. Willner, *Nat. Commun.*, 2012, **3**, 742
27 I. Vlassiouk and Z. S. Siwy, *Nano Lett.*, 2007, **7**, 552-556.

This journal is © The Royal Society of Chemistry 20xx

Please do not adjust margins